**Proceedings of ASME Turbo Expo 2011**
**GT2011**
**June 6-10, 2011, Vancouver, British Columbia, Canada**

**GT2011-45914**

# ASSESSMENT OF CURRENT CHEMILUMINESCENCE KINETICS MODELS AT ENGINE CONDITIONS

**Eric Petersen, Madeleine Kopp,** and **Nicole Donato**
Department of Mechanical Engineering
Texas A&M University, College Station, TX, USA

**Felix Güthe**
Combustion Technology Group
Alstom Power, Baden, Switzerland

## ABSTRACT

Chemiluminescence continues to be of interest as a cost-effective optical diagnostic for gas turbine combustor health monitoring. However, most chemical kinetics mechanisms of the chemiluminescence of target species such as OH*, CH*, and $CO_2$* were developed from atmospheric-pressure data. The present paper presents a study wherein the ability of current kinetics models to predict the chemiluminescence trends at engine pressures was assessed. Shock-tube experiments were performed in highly diluted mixtures of $H_2/O_2/Ar$ at a wide range of pressures to evaluate the ability of a current kinetics model to predict the measured trends. At elevated pressures up to 15 atm, the currently used reaction rate of H + O + M = OH* + M (i.e., without any pressure dependence) significantly over predicts the amount of OH* formed. Other important chemiluminescence species include CH* and $CO_2$*, and separate experiments were performed to assess the validity of existing chemical kinetics mechanisms for both of these species at elevated pressures. A pressure excursion using methane-oxygen mixtures highly diluted in argon was performed up to about 15 atm, and the time histories of CH* and $CO_2$* were measured over a range of temperatures from about 1700 to 2300 K. It was found that the existing CH* mechanism captured the T and P trends rather well, but the $CO_2$* mechanism did a poor job of capturing both the temperature and pressure behavior. With respect to the modeling of collider species, it was found that the current OH* model performs well for $N_2$, but some improvements can be made for $CO_2$.

## INTRODUCTION

The goal of the present study was to broaden the understanding of the chemical kinetics of species used in gas turbine applications for their chemiluminescence light intensities. Such efforts have been described in [1]. Making quantitative measurements of chemiluminescence species concentrations or even relative concentrations requires knowledge of the chemical kinetics of the molecules of interest. These species include OH*, CH*, $CO_2$*, and $C_2$*. Because of their small concentrations in the combustion zone (several orders of magnitude less than their ground-state counterparts), absolute measurements of the concentrations of the excited species are difficult. A shock tube is one way to produce the high temperatures seen in a gas turbine combustion zone, and it can be used as a model device for producing controlled conditions for obtaining time histories of excited species for kinetics model validation. Shock-tube experiments can also be used to obtain specific rate coefficients of key reactions in the formation and depletion of the excited species.

The present paper is concerned mainly with the assessment of and eventual improvement to the kinetics models for OH*, $CO_2$*, and CH* chemiluminescence. The work can be divided into the three parts: 1) OH* chemiluminescence at elevated pressure; 2) pressure effects on CH* and $CO_2$* chemiluminescence; and, 3) the effect of various collider species (M = $CO_2$, $N_2$) on OH* chemiluminescence. The following sections are divided into the same three parts, following a brief section on the experimental setup. Further details on the OH* results are in the thesis by Donato [2].

## EXPERIMENTAL SETUP

All experiments were performed in the shock-tube facility described by Aul [3]. This facility contains a 4.72-m driven section with a 15.24-cm internal diameter and a 4.92-m driver section with a 7.62-cm inner diameter. The inner diameter of the driver section is then expanded through a diverging section

 

to the driven diameter directly after the diaphragm location. The shock tube is made of 304 stainless steel. For every test, helium was used as the driver gas, and polycarbonate diaphragms were used for the lower-pressure experiments, and pre-scored aluminum diaphragms were used for the highest-pressure experiments.

High-purity gases were used to make the mixtures, which were all highly diluted in ultra high purity (UHP) argon (99.9995%). The oxygen and hydrogen were both UHP grade, and the methane was research grade (99.95%). The incident-shock velocity at the test region was found using five pressure transducers (PCB 113) set in series along the side of the shock tube which send signals to 4 Fluke PM 6666 time-interval counters. The incident-shock velocity was used with the standard one-dimensional shock relations to determine the conditions behind the reflected shock wave for each experiment.

Light emission from the chemiluminescence of OH*, CH*, or $CO_2$* was collected through two $CaF_2$ windows located at a sidewall location 1.0 cm from the endwall. For the CH* and $CO_2$* measurements, both emission signals were recorded simultaneously since the two windows were located on opposite sides of the driven tube. Two Hamamatsu 1P21 photomultiplier tubes (PMT) in custom-made enclosures were used to measure the emission through narrowband filters. Further details on the filter wavelengths and calibration of the optical setup are provided below.

## OH* CHEMILUMINESCENCE

These experiments focused on shock-tube mixtures of hydrogen and oxygen highly diluted in Argon, to isolate the contribution of the pressure-dependent reaction

$$H + O + M \rightleftarrows OH^* + M$$

to the formation of OH* (i.e., only H and O atoms available, with no hydrocarbons). We chose mixtures that had been used in prior experiments by the primary authors [4,5]. Once the optimal settings were obtained and experiments underway, it was necessary to validate the results with other data available in the literature. Petersen et al. [4] performed shock-tube experiments using the same mixture of $H_2/O_2/Ar$ with 98.5% dilution, $\phi = 1.0$, to examine the chemical kinetics of OH* ($A^2\Sigma^+ - X^2\Pi$) chemiluminescence in the temperature range from 1010—1750 K at low pressure. The shock tube used in the study by Petersen et al. [4] is similar to the one used in this study and is detailed in [5]. Since the optical settings differ between sets of experiments, it is necessary to normalize the data to a particular temperature and pressure, thus enabling a direct comparison of the data. A set of data was taken with the current setup to compare directly with the earlier data, and Fig. 1 verifies the repeatability of the low-pressure experimental results obtained by Petersen and co-workers.

Additionally, the experimentally obtained OH* profiles of this study were also compared to those of Petersen et al. [4] for cases of similar temperature. Figure 2 shows general agreement in the shape of the profiles between experiments. Slight differences can be attributed to the difference in temperature and the difference in optical settings. With low-pressure experiments validated against established data available in literature, the next major step was to perform a pressure excursion at 10 and 15 atm to obtain high-pressure data for the study herein and to evaluate the ability of currently used rates for OH* kinetics to capture the results seen in the new experiments at elevated pressure.

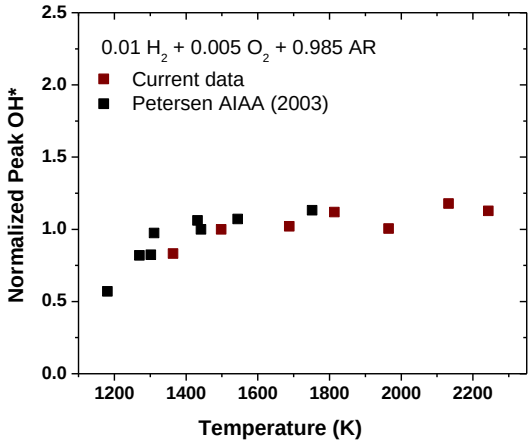


**Fig. 1** Maximum OH* concentration as a function of temperature at constant pressure and optical settings compared to the work of Petersen et al. [4]. Peak values are normalized to 1498 K and 1.15 atm.

The qualitative measurement of OH* chemiluminescence does not give a direct measure of the OH* concentration (mol/cm$^3$). Photomultiplier tube (PMT) output and OH* concentration are, however, proportional. Since the kinetics modeling of OH* at atmospheric pressure is well known [4], a calibration curve can be established using 1-atm experiments to extrapolate to conditions outside the range where the model has been verified. The calibration curve relates the PMT output (mV) to absolute concentration (mol/cm$^3$). A second set of low-pressure experiments was performed to cover a wide enough range of PMT output to create the calibration curve. The calibration mixture was $H_2/O_2/Ar$, $\phi = 1.0$ with 97% dilution, as opposed to 98.5% Ar dilution used in the rest of this work. The PMT output remains in the linear range over the range of the correlation used herein.

Finally, high-pressure experiments were performed at 10 and 15 atm over a wide range of temperatures. Comparisons of the

 

experimental results to the OH* model of Hall and Petersen [5] are shown in Fig. 3. Note that the base kinetics model for the $H_2$-$O_2$ chemistry is from the GRI 3.0 mechanism, and the simulations were performed using Chemkin [6]. Error bars are shown in Fig. 3 to represent the uncertainty in the value of the peak magnitude due to experimental repeatability from test to test, and was determined to be 10%. An uncertainty of ±10 K is associated with the experimental temperature determination. Although the model does a good job of predicting peak OH* formation at atmospheric pressure as expected, it significantly over predicts the peak concentration at higher pressures (10 and 15 atm). The model also shows a different trend than the data at the highest temperatures by predicting a decrease in peak OH*. In ongoing work, the experimental data in Fig. 3 and more like it are being used to obtain an improved model at elevated pressures.

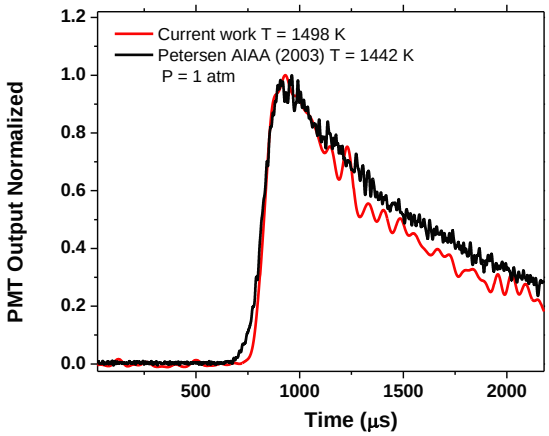


**Fig. 2** The normalized, experimentally obtained profile of OH* agrees well with the profile from Petersen et al. [4] at atmospheric pressure. Times have been adjusted to align OH* for comparison of the profile shape rather than the timing.

## $CO_2$* AND CH* CHEMILUMINESCENCE

Shock-tube experiments were performed in an argon-diluted methane/oxygen mixture to examine $CO_2$* and CH* at elevated pressures. $CO_2$* emission was captured using a narrow bandpass interference filter at 337 nm ±2 nm, while CH* emission was captured at 430 nm ± 5 nm, as shown in Fig. 4. Capturing the broadband emission of $CO_2$* with a 4-nm bandpass filter is adequate since any portion of the spectrum should be due to the excited state of $CO_2$; that is, a measurement focused at 400 nm should give time-specific results similar to those at 337 nm, just at a higher overall intensity.

We are however assuming herein that the broad background seen in Fig. 4 is due primarily to $CO_2$*, an assumption which is commonly made but is nonetheless a hypothesis. For example, Mancaruso and Vaglieco [7] in diesel engine emission spectroscopy experiments attribute emission in the same region to excited states of HCO and HCHO. They also used a narrowband filter centered near 330 nm but linked this to a slice of the broader HCO spectroscopic feature. Confirmation of the source of the broadband emission in the blue region of the spectrum for gas turbine conditions and for the measurements of interest herein will have to be made in a later study.

The overall chemiluminescence reaction for $CO_2$* is given by:

$$CO + O \rightleftarrows CO_2 + h\nu \qquad \text{(R0)}$$

Where the chemiluminescence intensity, I, is:

$$I = I_o\,[CO]\,[O]$$

The formation and depletion of $CO_2$* can be shown by the following three steps:

$$CO + O + M \rightleftarrows CO_2^* + M \qquad \text{(R1)}$$

$$CO_2^* \rightleftarrows CO_2 + h\nu \qquad \text{(R2)}$$

$$CO_2^* + M \rightleftarrows CO_2 + M \qquad \text{(R3)}$$

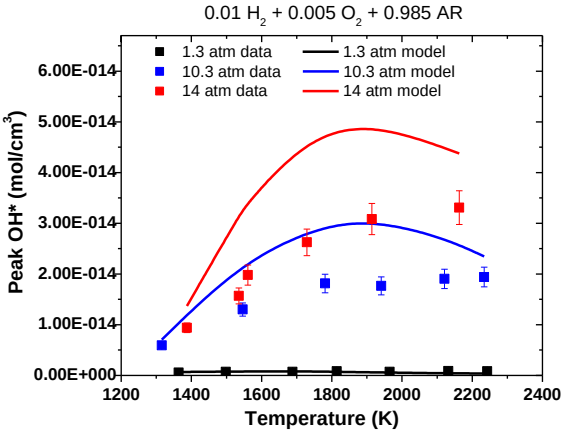


**Fig. 3** Comparison of OH* mechanism and data at three different pressures. The model predictions (lines) significantly over predict the experimental results at elevated pressures.

These reactions yield a rate coefficient, $I_o = (K_1K_2)/K_3$. To date, there exists no detailed $CO_2$* mechanism. Rather, the photon emission rate, $i_{CO2*}$, is given by a global rate that is dependent on the concentrations of [CO] and [O]. This global rate is given by Slack et al. [8] and recently used by Nori and Seitzman [9] as:

$$i_{CO2*} = 3.3(\pm 0.3)\times 10^3 \exp(-2300/T)[CO][O]$$

where temperature is in K, and species concentrations are in units of mol/cm$^3$.

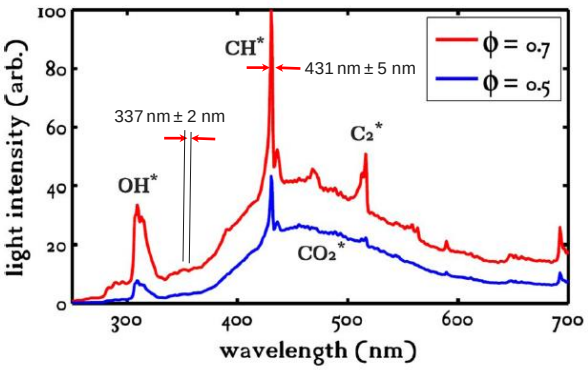


**Fig. 4** Chemiluminescence spectrum pointing out the wavelengths at which $CO_2$* and CH* were captured.

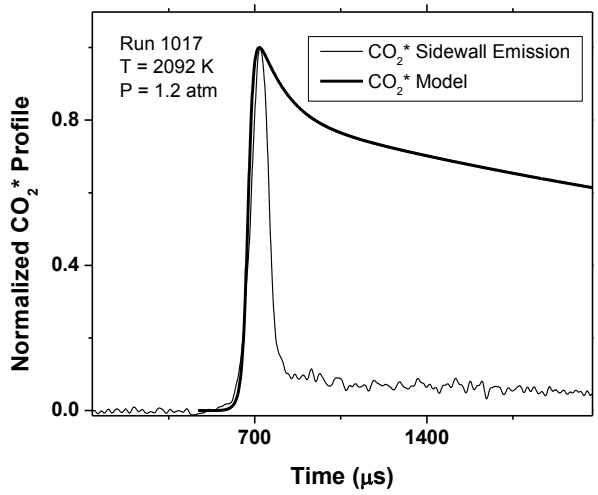


**(a)** $CO_2$* profiles at P = 1.2 atm

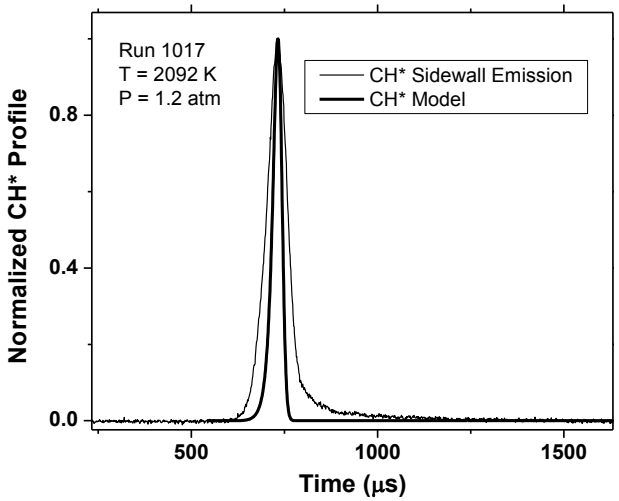


**(b)** CH* profiles at P = 1.2 atm

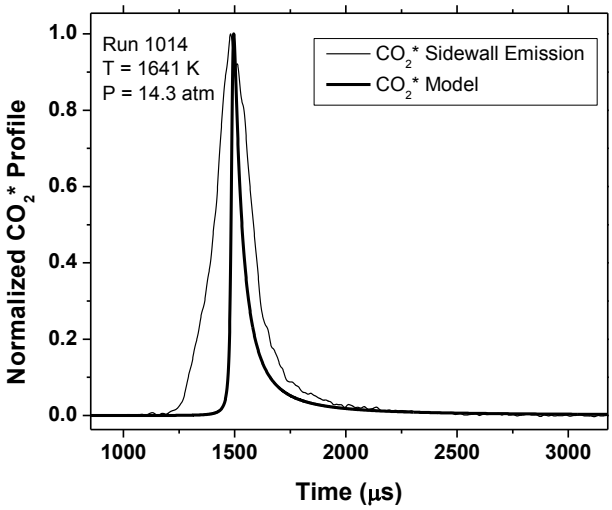


**(c)** $CO_2$* profiles at P = 14.3 atm

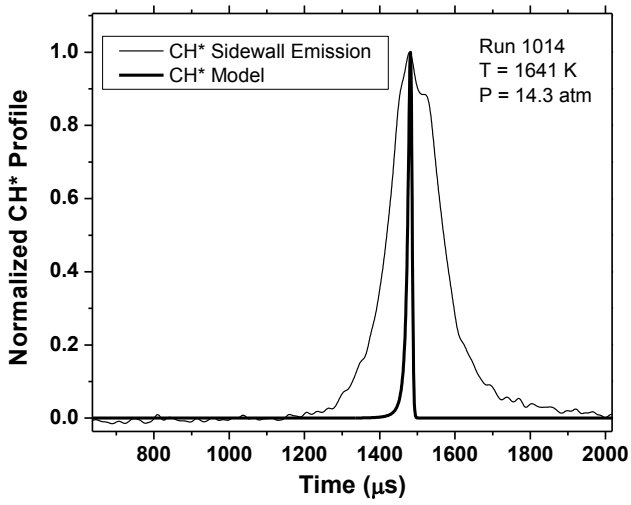


**(d)** CH* profiles at P = 14.3 atm

**Fig. 5** Representative profiles from stoichiometric methane/oxygen mixtures in 99.1% Ar are compared to model profiles for $CO_2$* and CH*. Calculations are adjusted in time so that the times of peak concentration coincide with the measured results.

The detailed mechanism used to model CH* was taken from de Vries et al. [10], where CH* is formed by the following reactions:

$$C_2H + O \rightleftarrows CO + CH^*$$

$$C_2 + OH \rightleftarrows CO + CH^*$$

$$C + H + M \rightleftarrows CH^* + M$$

The depletion of CH* occurs by way of the following reactions:

$$CH^* \rightleftarrows CH + h\nu$$

$$CH^* + M \rightleftarrows CH + M$$

Where M represents possible collider species: Ar, $N_2$, $H_2O$, $H_2$, $O_2$, CO, $CO_2$, and $CH_4$.

Figure 5 compares the model-predicted profiles to the experimentally obtained profiles for $CO_2$* and CH* at both atmospheric (1.2 atm) and elevated (14.3 atm) pressures. The mixture used in this study was a stoichiometric mixture of $CH_4/O_2$ diluted in 99.1% Argon. The current state of the global rate used to model $CO_2$* does not accurately capture the profile obtained experimentally. This disagreement is largely due to the fact that the profile is dependent on the concentrations of [CO] and [O]. Comparing Fig. 5a to the profiles of [CO] and [O] shown in Fig. 6a, it is seen that $CO_2$* follows the same trend as the concentration of CO times the concentration of O. A similar trend is seen when comparing the results of the higher-pressure (14.3 atm) case in Fig. 5c to the calculated [CO], [O], and [CO]×[O] time histories at the same temperature and pressure in Fig. 6b. In contrast, CH* profiles are predicted reasonably well by the model, but with the model predicting a much narrower profile at high pressure.

In addition to examining the profile shapes of $CO_2$* and CH*, the peak values predicted by the model were compared to experimentally obtained peaks. The peak values were normalized to a particular temperature and pressure for comparison purposes. Peak CH* concentration values predicted by the model accurately match the peak values seen experimentally as a function of temperature. The correct temperature and pressure trends were captured by the model (Fig. 7).

While excellent agreement was seen in predicting CH* peak values, the same agreement was not observed with $CO_2$*. Figure 8 shows that the model fails to predict both the temperature and pressure trends. At low pressure, the model shows a near-constant peak value regardless of the temperature, while the experiment shows increasing peak values with increasing temperature. At high pressure, the model significantly over predicts the peak $CO_2$* observed experimentally. Thus, there exists a need to develop a detailed mechanism for $CO_2$*. The first step in this process would be to determine the reaction rate for the following pressure-dependent reaction:

$$CO + O + M \rightleftarrows CO_2^* + M$$

Future experiments are planned to determine the rate coefficient for this reaction and a better overall chemical kinetics model for $CO_2$*. There is also the possibility of additional pathways for $CO_2$* formation that are not considered in the crude and virtually untested $CO_2$* mechanism employed herein. Some possibilities might include reactions where CO acts as a third body and bimolecular collisions that could be energetic enough to excite $CO_2$ to $CO_2$*.

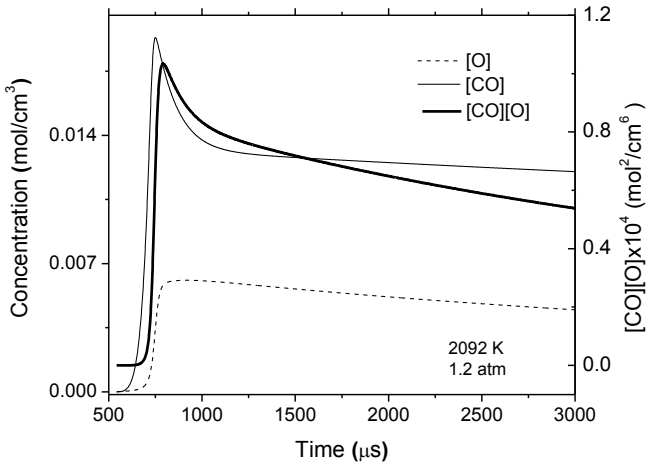


**(a)** 2092 K, 1.2 atm

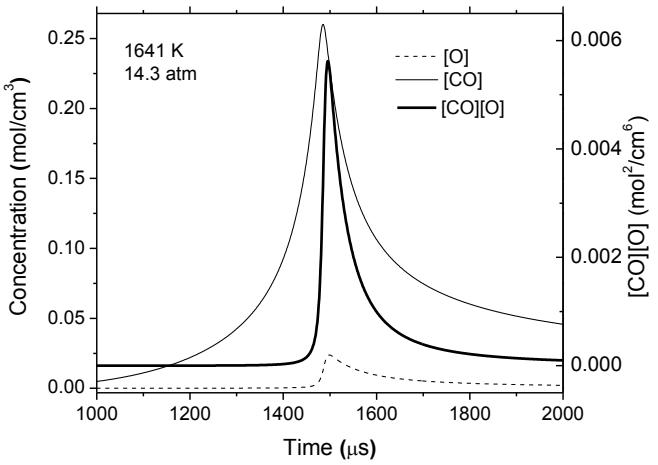


**(b)** 1641 K, 14.3 atm

**Fig. 6** The product of the CO concentration times the O concentration dictates the overall profile shape of $CO_2$*. Results here are calculated from the kinetics model (GRI 3.0) for the stoichiometric $CH_4$-$O_2$ mixture in 99.1% Ar.

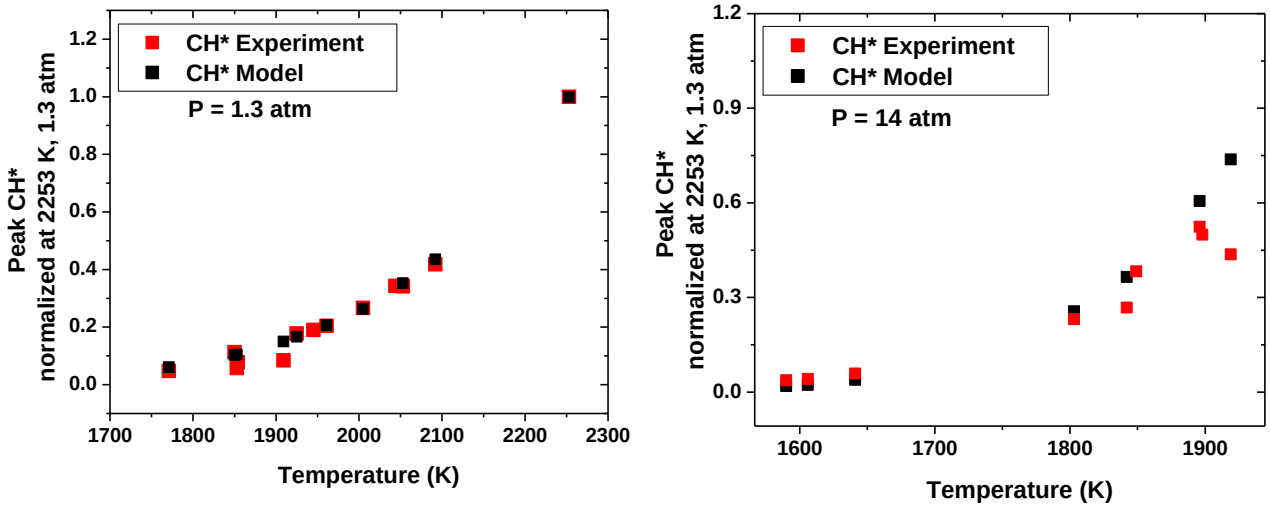


**Fig. 7** Peak concentration of CH* is compared to the peak value obtained experimentally at atmospheric (left) and elevated (right) pressures with excellent agreement.

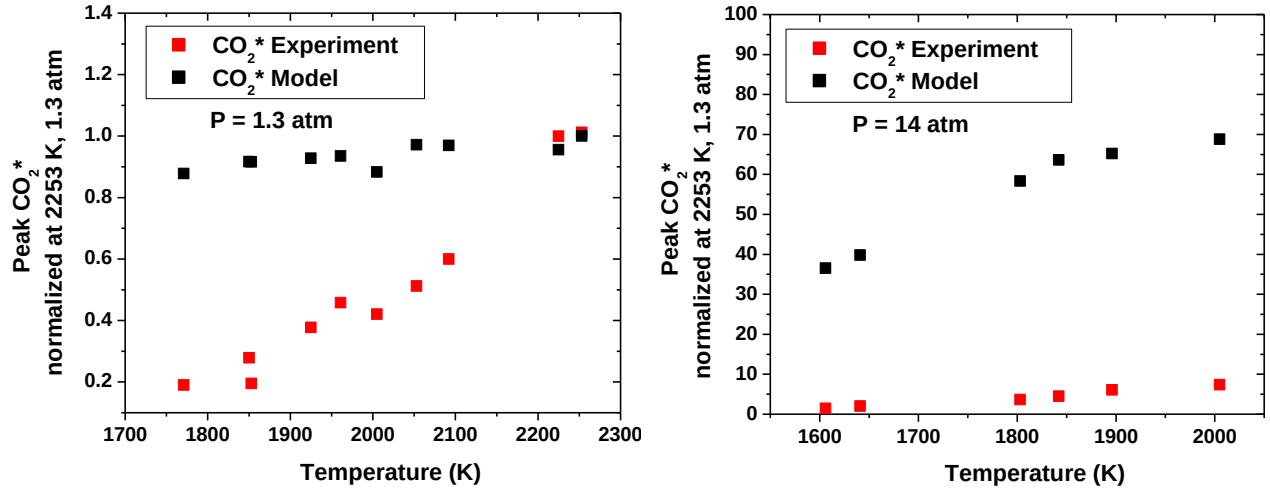


**Fig. 8** Predicted peak concentration of $CO_2$* is compared to the peak value obtained experimentally. Poor agreement is seen at atmospheric (left) and elevated (right) pressures.

## EFFECT OF COLLIDER SPECIES

A separate series of experiments was conducted to determine how well the OH* model performed when collider species other than argon were present in significant quantities. Two mixtures were utilized for this part of the study. The first mixture was a stoichiometric $H_2$-$O_2$ mixture in a nitrogen bath gas with 97% by volume $N_2$. The second mixture contained $CO_2$ in the following blend: 0.006 $H_2$ + 0.003 $O_2$ + 0.05 $CO_2$ + 0.941 Ar. Note that a test mixture containing only carbon dioxide as the bath gas species is not practical in a reflected-shock experiment due to the nonideal effects that would exist with the mostly triatomic mixture [11].

Figure 9 shows two examples of OH* time histories for the $N_2$ bath gas, one at 1208 K and the other at 1272 K, both at a pressure of 1.1 atm. In both cases seen in Fig. 9, the model does a **good** job at predicting the rise and decay of the OH* concentration at this low-pressure condition. There is a slight overprediction of the decay by the model which is almost within the signal-to-noise of the data trace. Therefore, there could be room for slight improvements in the $N_2$ collider kinetics, but the current performance is probably acceptable for most applications. Due to the inadequacies of the high-pressure OH* chemistry highlighted in Fig. 3, pressures higher than about 1 atm were not included in this collider species study.

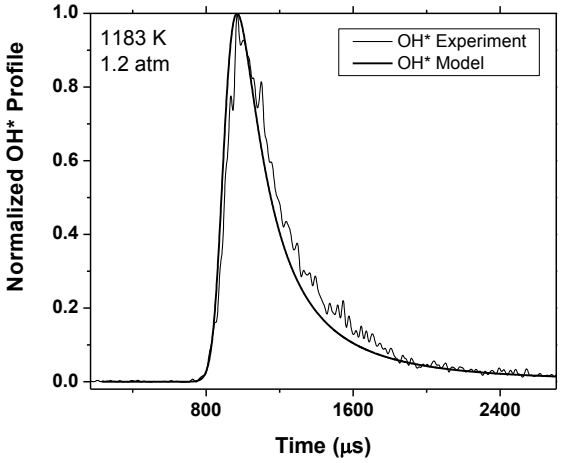


**(a)** OH* time histories for 1183 K, 1.2 atm

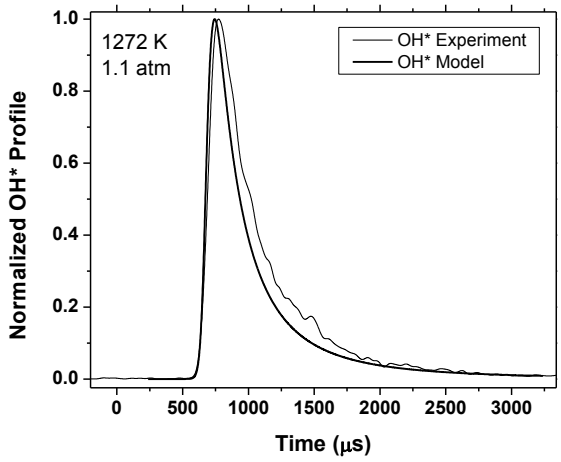


**(b)** OH* time histories for 1272 K, 1.1 atm

**Fig. 9** Predicted and measured OH* for the nitrogen-based mixture, 2% $H_2$ + 1% $O_2$ + 97% $N_2$.

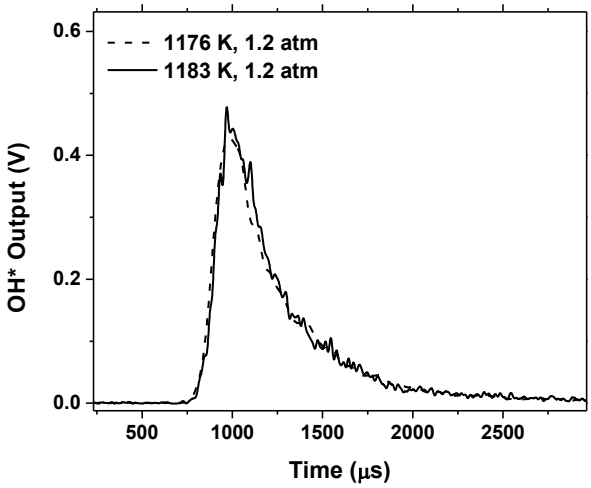


**Fig. 10** Repeatability of measured OH* for the nitrogen-based mixture, 2% $H_2$ + 1% $O_2$ + 97% $N_2$.

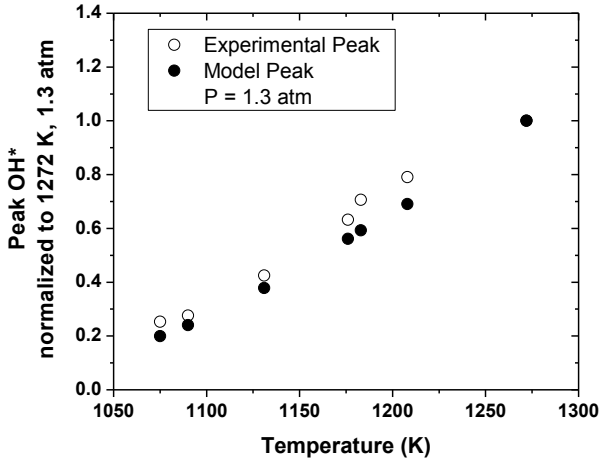


**Fig. 11** Peak OH* concentration normalized to the result at 1272 K over a range of temperature for the nitrogen-based mixture, 2% $H_2$ + 1% $O_2$ + 97% $N_2$. Both model and experiment are shown.

The repeatability of the nitrogen-bath experiments was quite good, as seen in Fig. 10 for two different tests at nearly the same temperatures (1183 and 1176 K). For the entire series of experiments with the 97% $N_2$ mixture between about 1070 and 1270 K, the peak concentration of OH* can be compared. Figure 11 shows the peak OH* concentration normalized to the concentration obtained at 1272 K for both the experiment and the model. Both sets of points in Fig. 11 are in fair agreement, indicating that the kinetics model does an adequate job at predicting the behavior with nitrogen as the collider species.

Comparisons between model and experiment for the mixture containing $CO_2$ are shown in Figs. 12 and 13 for the OH* time history and peak concentration, respectively. As seen in Fig. 12 for the representative OH* time history, the model tends to overpredict the decay rate of OH* relative to the measured results, indicating that some improvement in the model with respect to $CO_2$ as a collider species can be made in the future. However, when comparing the peak OH* concentration over the measured range of temperatures (about 1300 to 2200 K), the model seems to perform fairly well (Fig. 13) but

 

overpredicts the peak concentration near 1500 K and under predicts it for temperatures above about 1900 K. A detailed sensitivity analysis would shed more insight into the discrepancies seen in Fig. 13 and should therefore be performed in the follow-up work to the present study.

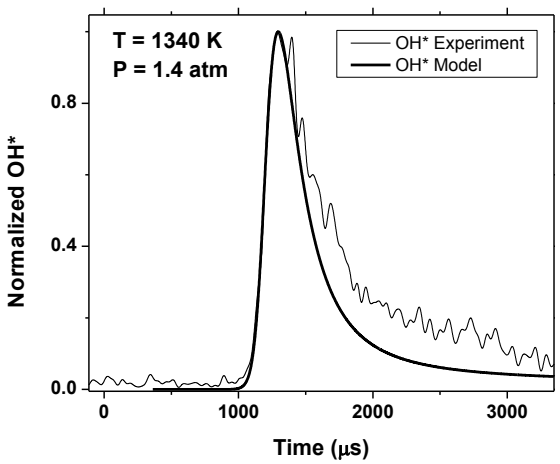


**Fig. 12** Modeled and measured OH* time history for the mixture containing $CO_2$: 0.6% $H_2$ + 0.3% $O_2$ + 5% $CO_2$ + 94.1% Ar. Note that the model tends to overpredict slightly the decay rate of OH*.

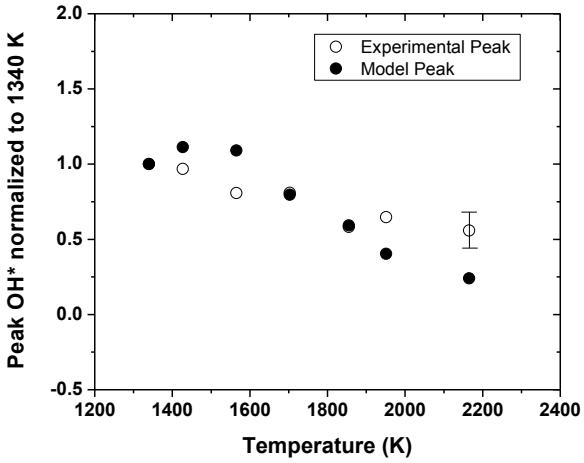


**Fig. 13** Calculated and measured peak OH* concentration for the mixture containing $CO_2$: 0.6% $H_2$ + 0.3% $O_2$ + 5% $CO_2$ + 94.1% Ar over a range of temperatures. The peak values are normalized to the concentration at 1340 K. Typical error bars are shown on the highest-temperature point.

Finally, it is of interest to compare the temperature trends observed using the peak level of OH* to the trends observed when the full width of the concentration history is utilized. Figure 14 shows the comparison between the normalized peak values to the normalized areas under the profiles of OH* time histories calculated using the model. One can infer from Fig. 14 that the same temperature trend is observed whether the peak or full area of the OH* is used, at least for the range of conditions measured herein for the lower-pressure cases near 1 atm.

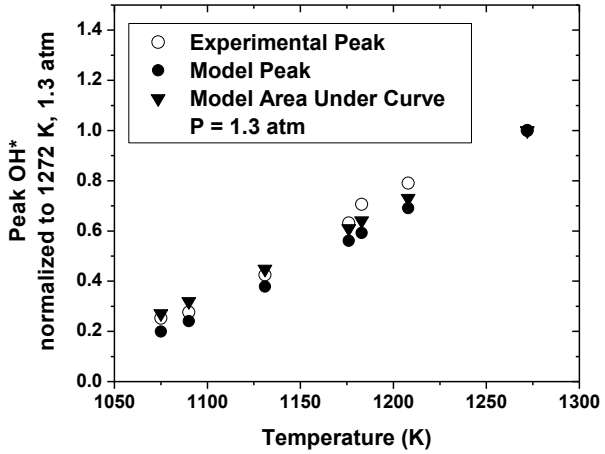


**Fig. 14** Comparison of peak concentration to the normalized area under the entire OH* time history for the nitrogen-based mixture with 97% $N_2$. Values are normalized to the 1272 K, 1.3-atm results.

## SUMMARY

Shock-tube experiments and kinetics modeling were performed to assess the chemiluminescence kinetics of OH*, $CO_2$*, and CH* at gas turbine pressures and temperatures. In the first part, the pressure dependence of the key OH* formation reaction O + H + M ⇄ OH* + M was assessed at pressures up to 14 atm using $H_2$-$O_2$ mixtures highly diluted in argon. These measurements involved a careful set of experiments that utilized a calibration based on the assumed kinetics of OH* at 1 atm. A second set of experiments was performed to assess the kinetics models of $CO_2$* and CH* at elevated pressures. The results of this pressure excursion using methane-oxygen mixtures in argon was that the CH* mechanism is good at capturing the temperature and pressure trends, while the $CO_2$* model is as defined herein rather poor. Finally, measurements utilizing mixtures containing large levels of $N_2$ or $CO_2$ were performed, and it was found that the model does a good job with nitrogen species at the conditions studied (1 atm) for OH*. For the mixture containing $CO_2$, some improvements are warranted since the model tends to overpredict the decay rate of the OH*.

One can conclude from this study that improvements should be made to the $CO_2$* mechanism, including its pressure dependence via the reaction CO + O + M ⇄ $CO_2$* + M, as well as an assessment of whether additional reactions are needed. A similar conclusion can be drawn for the OH* pressure

 

dependence, and further work should be done to assess the validity of the OH* mechanism in the presence of hydrocarbons at elevated pressures. In future work, the effect of collider species $N_2$ and $CO_2$ (and perhaps $H_2O$) on the kinetics of CH* and $CO_2$* should also be assessed.

## ACKNOWLEDGMENTS

This work was supported by Alstom Power, Baden, Switzerland.

## REFERENCES

[1] Schuermans, B., Guethe, F., Pennell, D., Guyot, D., Paschereit, O. C., 2010 "Thermoacoustic Modeling of a Gas Turbine Using Transfer Functions Measured Under Full Engine Pressure," Journal of Engineering for Gas Turbines and Power 132, 111503.

[2] Donato, N. S., 2009 "OH* Chemiluminescence: Pressure Dependence of H+O+M = OH*+M," M.S. Thesis, Texas A&M University.

[3] Aul, C. J., 2009 "An Experimental Study into the Ignition of Methane and Ethane Blends in a New Shock-Tube Facility," M.S. Thesis, Texas A&M University.

[4] Petersen, E. L., Kalitan, D. M., and Rickard, M. J. A., 2003 "Calibration and Chemical Kinetics Modeling of an OH Chemiluminescence Diagnostic," AIAA paper 2003-4493.

[5] Hall, J. M. and Petersen, E. L., 2006 "An Optimized Kinetics Model for OH Chemiluminescence at High Temperatures and Atmospheric Pressures," International Journal of Chemical Kinetics 38, pp. 714-724.

[6] Kee, R. J., Rupley, F. M., Miller, J. A., Coltrin, M. E., Grcar, J. F., Meeks, E., Moffat, H. K., Lutz, A. E., Dixon-Lewis, G., Smooke, M. D., Warnatz, J., Evans, G. H., Larson, R. S., Mitchell, R. E., Petzold, L. R., Reynolds, W. C., Caracotsios, M., Stewart, W. E., Glarborg, P., Wang, C., and Adigun, O., 2000. Chemkin Collection. San Diego, CA: Release 3.6, Reaction Design, Inc.

[7] Mancaruso, E., Vaglieco, B. M. 2011 "Spectroscopic Measurements of Premixed Combustion in Diesel Engine," Fuel 90, 511-520.

[8] Slack, M. and Grillo, A., 1985 "High Temperature Rate Coefficient Measurements of CO+O Chemiluminescence," Combustion and Flame 59, pp. 189-196.

[9] Nori, V. and Seitzman, J., 2008 "Evaluation of Chemiluminescence as a Combustion Diagnostic under Varying Operating Conditions," AIAA Paper 2008-0953.

[10] de Vries, J., Hall, J. M., Simmons, S. L., Rickard, M. J. A., Kalitan, D. M., and Petersen, E. L., 2007 "Ethane Ignition and Oxidation behind Reflected Shock Waves," Combustion and Flame 150, pp. 137-150.

[11] Petersen, E. L. and Hanson, R. K., 2006 "Measurements of Reflected-Shock Bifurcation Over a Wide Range of Gas Composition and Pressure," Shock Waves 15, pp. 333-340.

 